

Few-body bound states of two-dimensional bosons

G. Gujarro , G. E. Astrakharchik , and J. Boronat 

Departament de Física, Campus Nord B4-B5, Universitat Politècnica de Catalunya, E-08034 Barcelona, Spain

B. Bazak 

Racah Institute of Physics, Hebrew University, 9190401 Jerusalem, Israel

D. S. Petrov 

Université Paris-Saclay, CNRS, LPTMS, 91405 Orsay, France



(Received 5 November 2019; accepted 11 March 2020; published 7 April 2020)

We study clusters of the type $A_N B_M$ with $N \leq M \leq 3$ in a two-dimensional mixture of A and B bosons, with attractive AB and equally repulsive AA and BB interactions. In order to check universal aspects of the problem, we choose two very different models: dipolar bosons in a bilayer geometry and particles interacting via separable Gaussian potentials. We find that all the considered clusters are bound and that their energies are universal functions of the scattering lengths a_{AB} and $a_{AA} = a_{BB}$, for sufficiently large attraction-to-repulsion ratios a_{AB}/a_{BB} . When a_{AB}/a_{BB} decreases below ≈ 10 , the dimer-dimer interaction changes from attractive to repulsive and the population-balanced $AABB$ and $AAABBB$ clusters break into AB dimers. Calculating the $AAABBB$ hexamer energy just below this threshold, we find an effective three-dimer repulsion which may have important implications for the many-body problem, particularly for observing liquid and supersolid states of dipolar dimers in the bilayer geometry. The population-imbalanced ABB trimer, $ABBB$ tetramer, and $AABBB$ pentamer remain bound beyond the dimer-dimer threshold. In the dipolar model, they break up at $a_{AB} \approx 2a_{BB}$, where the atom-dimer interaction switches to repulsion.

DOI: [10.1103/PhysRevA.101.041602](https://doi.org/10.1103/PhysRevA.101.041602)

Recent experiments on dilute quantum droplets in dipolar bosonic gases [1–4] and in Bose-Bose mixtures [5–7] with competing interactions have exposed the important role of beyond-mean-field effects in weakly interacting systems. A natural strategy to boost these effects and enhance exotic behaviors is to make the interactions stronger while keeping the attraction-repulsion balance for mechanical stability. The most straightforward way of getting into this regime is to increase the gas parameter na_s^3 . However, this leads to enhanced three-body losses, which results in very short lifetimes (as has been observed in experiments [1–7]). Nevertheless, this regime is achievable in reduced geometries. It has been shown that a one-dimensional Bose-Bose mixture with strongly attractive interspecies interaction becomes dimerized and, by increasing the intraspecies repulsion, the dimer-dimer interaction can be tuned from attractive to repulsive [8]. Then, an effective three-dimer repulsion has been found in this system and predicted to stabilize a liquid phase of attractive dimers [9].

In two dimensions, a particularly interesting realization of such a strongly interacting, tunable, and long-lived Bose-Bose mixture is a system of dipolar bosons confined to a bilayer geometry [10–12]. When the dipoles are oriented perpendicularly to the plane, there is a competing effect between repulsive intralayer and partially attractive interlayer interactions, interesting from the viewpoint of liquid formation. In addition, the quasi-long-range character of the dipolar interaction can produce the rotonization of its spectrum and

a supersolid behavior [13–21], formation of a crystal phase [22,23], and a pair superfluid [24–26] (see also lattice calculations of Ref. [27]). A peculiar feature of bilayer model is the vanishing Born integral for the interlayer interaction, $\int V_{AB}(\rho)d^2\rho = 0$ [28], which has led to controversial claims about the existence of a two-body bound state [29] until it has finally been established that this bound state always exists, although its energy can be exponentially small [30–34], consistent with Ref. [35]. Interestingly, a similar controversy seems to continue at the few-body level; it has been claimed [36] that the repulsive dipolar tails will never allow for three- or four-body bound states in this geometry.

In this Rapid Communication, we investigate few-body bound states in a two-dimensional mass-balanced mixture of A and B bosons with two types of interactions characterized by the two-dimensional scattering lengths a_{AB} and $a_{AA} = a_{BB}$. The first case corresponds to the bilayer of dipoles discussed above and, in the second, we model the interactions by non-local (separable) finite-range Gaussian potentials. By using the diffusion Monte Carlo (DMC) technique in the first case, and the stochastic variational method (SVM) in the second, we find that for sufficiently weak BB repulsion compared to the AB attraction, $a_{AB} \gg a_{BB}$, all clusters of the type $A_N B_M$ with $1 \leq N \leq M \leq 3$ are bound. We then locate thresholds for their unbinding with decreasing a_{AB}/a_{BB} . By looking at the $AAABBB$ hexamer energy close to the corresponding threshold, we discover an effective three-dimer repulsion, which can stabilize interesting many-body phases.

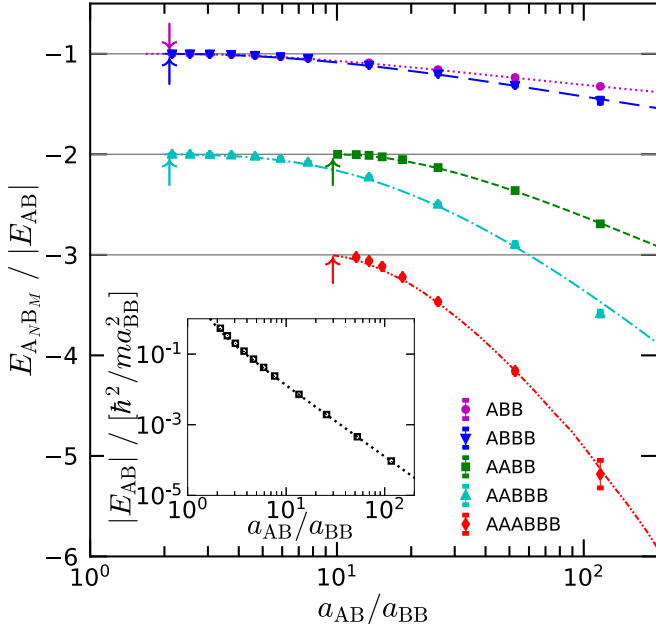


FIG. 1. Energies of $A_N B_M$ clusters in units of the dimer energy E_{AB} (reported in the inset in units of $\hbar^2/m a_{BB}^2$) for Gaussian (curves) and dipolar (symbols) potentials as a function of the scattering length ratio a_{AB}/a_{BB} . The arrows show the positions of the thresholds for binding in the dipolar case.

The Hamiltonian of our system is given by

$$\hat{H} = -\frac{\hbar^2}{2m} \sum_{i=1}^N \nabla_i^2 - \frac{\hbar^2}{2m} \sum_{\alpha=1}^M \nabla_\alpha^2 + \sum_{i<j} \hat{V}_{AA}(r_{ij}) + \sum_{\alpha<\beta} \hat{V}_{BB}(r_{\alpha\beta}) + \sum_{i,\alpha} \hat{V}_{AB}(r_{i\alpha}), \quad (1)$$

where the two-dimensional vectors \mathbf{r}_i and \mathbf{r}_α denote particle positions of species A and B containing, respectively, N and M atoms, \hat{V}_{AB} and $\hat{V}_{AA} = \hat{V}_{BB}$ are the interspecies and intraspecies interaction potentials, and m is the mass of each particle. For the bilayer setup, we have $V_{AA}(r) = V_{BB}(r) = d^2/r^3$ and $V_{AB}(r) = d^2(r^2 - 2h^2)/(r^2 + h^2)^{5/2}$, where d is the dipole moment and h is the distance between the layers. Dipoles are aligned perpendicularly to the layers and there is no interlayer tunneling. The potential $V_{BB}(r)$ is purely repulsive and is characterized by the h -independent scattering length $a_{BB} = e^{2\gamma} r_0$ [37], where $\gamma \approx 0.577$ is the Euler constant and $r_0 = m d^2 / \hbar^2$ is the dipolar length. The interlayer potential $V_{AB}(r)$ always supports at least one dimer state. Its energy reported in the inset of Fig. 1 diverges for $h \rightarrow 0$ and exponentially vanishes in the opposite limit [30–33]. The scattering length a_{AB} , which is a function of r_0 and h , is $\sim a_{BB} \sim r_0$ for $h \sim r_0$, and exponentially large for $h \gg r_0$. In the following, we parametrize the system by specifying a_{BB} and a_{AB} rather than h and r_0 .

In the more academic case of Gaussian interactions, we use $\hat{V}_{AB}(r_{i\alpha})\psi(r_{i\alpha}) = \int V_{AB}(r_{i\alpha}, r'_{i\alpha})\psi(r'_{i\alpha})d^2r'_{i\alpha}$ and similarly for V_{AA} and V_{BB} , where $V_{\sigma\sigma'}(r, r') = C_{\sigma\sigma'} G_\xi(r)G_\xi(r')$, $G_\xi(r) = (2\pi\xi^2)^{-1} \exp(-r^2/2\xi^2)$, and ξ is the characteristic range of the potential. An advantage of this nonlocal potential is that the two-body problem can be solved analytically, giving

$C_{\sigma\sigma'}^{-1} = \frac{m}{4\pi\hbar^2} [2 \ln \frac{2\xi}{a_{\sigma\sigma'}} - \gamma]$. In the following, we vary the ratio a_{AB}/a_{BB} , with $a_{BB} = 1.4\xi$ fixed. Note that the available ratio is limited to $a_{AB}/a_{BB} > 1.1$.

In order to calculate the energies of the different few-body clusters, we employ two numerical techniques. In the dipolar case, we use the diffusion Monte Carlo (DMC) method [38], which leads to the exact ground-state energy of the system, within a statistical error. This stochastic technique solves the Schrödinger equation in imaginary time using a trial wave function for importance sampling. We choose it to be

$$\Psi_T(\mathbf{r}_1, \dots, \mathbf{r}_{N+M}) = \prod_{i<j}^N f_{AA}(r_{ij}) \prod_{\alpha<\beta}^M f_{BB}(r_{\alpha\beta}) \times \left[\prod_{i=1}^N \sum_{\alpha=1}^M f_{AB}(r_{i\alpha}) + \prod_{\alpha=1}^M \sum_{i=1}^N f_{AB}(r_{i\alpha}) \right].$$

The interspecies correlations are described by the dimer wave function $f_{AB}(r)$, calculated numerically, and the intraspecies Jastrow factors are chosen as the zero-energy two-body scattering solution, $f_{AA}(r) = f_{BB}(r) = K_0(2\sqrt{r_0/r})$, with K_0 being the modified Bessel function.

In the Gaussian model, we use the stochastic variational method (SVM) [39], where the wave function is expanded in a correlated Gaussian basis $\Psi(\eta) = \sum_i c_i \hat{S} \exp(-\frac{1}{2}\eta^T A_i \eta)$, where η is the vector of $N + M - 1$ particle coordinates in the center-of-mass reference frame and the matrices A_i are real, symmetric, and positive definite. \hat{S} is the symmetrization operator, relevant for our Bose-Bose mixture, and the index i sums over the basis functions (with ≈ 3000 functions). The Schrödinger equation is then reduced to a generalized eigenvalue problem, giving the expansion coefficients $\{c_i\}$ and the corresponding energy. The basis is optimized to the system at hand in a stochastic way, where elements of the matrices A_i are chosen randomly taking at each step the element that gives the lowest energy. Our SVM implementation closely follows Ref. [40].

We first discuss the limit of very large a_{AB} (large dimer size) when the interaction range and the intraspecies interactions can be neglected. In this case, the problem can be treated in the zero-range approximation giving for the ABB trimer $E_{ABB}^{a_{BB}=0} = 2.39E_{AB}$ [41–43] and for the tetramers $E_{ABBB}^{a_{BB}=0} = 4.1E_{AB}$ and $E_{AABB}^{a_{BB}=0} = 10.6E_{AB}$ [41]. Here, we find that the other $A_N B_M$ clusters (with $1 \leq N \leq M \leq 3$) are also bound in absence of the intraspecies repulsion. Using the method of Ref. [44], we calculate their binding energies (and also update the energies of smaller clusters): $E_{ABB}^{a_{BB}=0}/E_{AB} = 2.3896(1)$, $E_{ABBB}^{a_{BB}=0}/E_{AB} = 4.1364(2)$, $E_{AABB}^{a_{BB}=0}/E_{AB} = 10.690(2)$, $E_{AABBB}^{a_{BB}=0}/E_{AB} = 28.282(5)$, and $E_{AAABBB}^{a_{BB}=0}/E_{AB} = 104.01(5)$.

The intraspecies repulsion shifts the cluster energies upward as has been seen for the ABB trimer [45,46] and the $ABBB$ tetramer [46]. In Fig. 1, we report the energies of these and bigger clusters for both the dipolar and Gaussian interactions. Note that even for the weakest BB repulsion shown in this figure ($a_{AB}/a_{BB} = 200$), the clusters are significantly less bound compared to the case of no BB repulsion. This happens since the small parameter that controls the weakness of the intraspecies interaction relative to the interspecies one

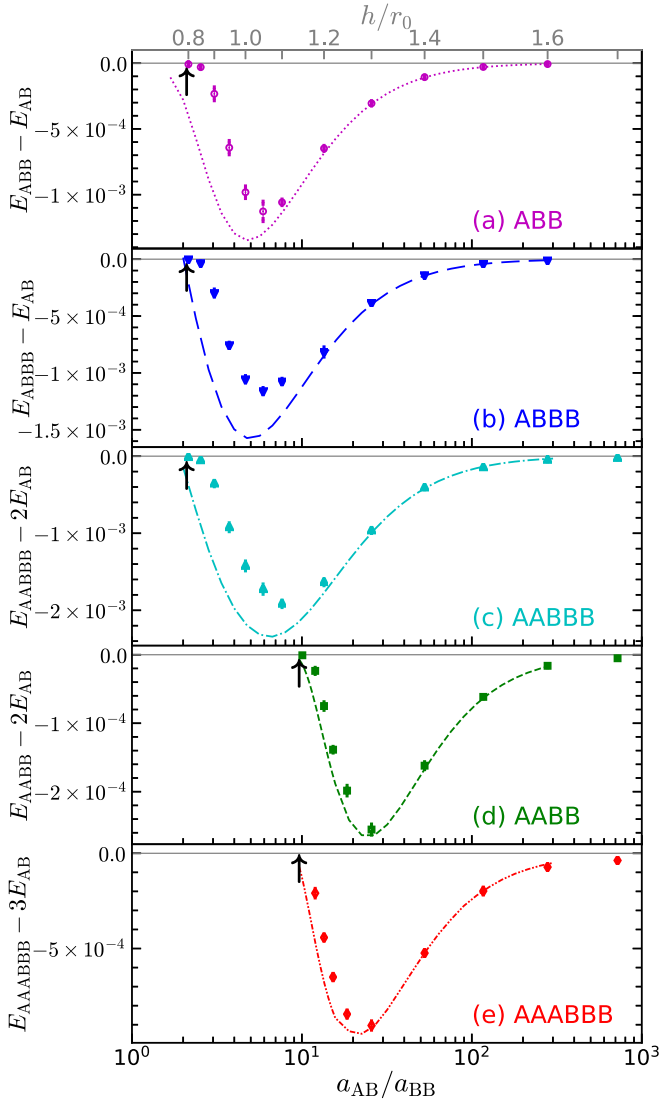


FIG. 2. Binding energies of the few-body clusters $E_{A_n B_m} - nE_{AB}$, in units of $\hbar^2/m a_{BB}^2$, vs a_{AB}/a_{BB} , for Gaussian (curves) and dipolar (symbols) potentials.

is actually $\lambda = 1/\ln(a_{AB}/a_{BB}) \ll 1$. By contrast, effective-range corrections contain powers of $r_0\sqrt{mE}/\hbar$ or $\xi\sqrt{mE}/\hbar$ for dipolar or Gaussian interactions, respectively, which are exponentially small in terms of λ . This explains why the two interaction models lead to almost indistinguishable results for large a_{AB}/a_{BB} .

We find that for sufficiently strong intraspecies repulsion (smaller a_{AB}/a_{BB}) the trimer and all higher clusters get unbound. In Fig. 1, the thresholds for binding in the dipolar model are shown by arrows. We find that the tetramer threshold is located at $a_{AB}/a_{BB} \approx 10$ ($h/r_0 \approx 1.1$) and the trimer threshold, corresponding to the atom-dimer zero crossing, occurs in the regime where all relevant length scales (scattering lengths, dimer sizes, interaction ranges) are comparable to one another; $a_{AB}/a_{BB} \approx 2$ ($h/r_0 \approx 0.8$) for the dipolar model. The positions of the threshold and differences between the results of the two models are better visible in Fig. 2, where we plot the cluster energies in units of $\hbar^2/m a_{BB}^2$. The threshold values are obtained by fitting the energy results to

the function $E_{A_n B_m} - nE_{AB} = E_0 \exp\{-1/[c_1(a_{AB} - a_{AB}^c) + c_2(a_{AB} - a_{AB}^c)^2]\}$, for $a_{AB} > a_{AB}^c$, where a_{AB}^c , E_0 , c_1 , c_2 are free parameters.

Our numerical calculations for larger clusters indicate that, depending on whether they are balanced ($M = N$) or not, their unbinding thresholds coincide, respectively, with the tetramer or with the trimer ones. To understand these results, note that close to these thresholds the clusters are much larger than the dimer. Treating there the latter as an elementary boson D , the $AABBB$ pentamer and the $ABBB$ tetramer can be thought of as weakly bound DDB or DBB “trimers” characterized by a large a_{DB} value and repulsive DD and BB interactions (the DD interaction is repulsive since we are above the tetramer $AABB$ threshold). In the limit $a_{DB} \rightarrow \infty$, the DD and BB interactions can be neglected and the binding energies of the DDB and DBB composite trimers are asymptotically fractions of $E_{ABB} - E_{AB}$ [42]. The ABB trimer, $ABBB$ tetramer, and $AABBB$ pentamer thresholds are therefore the same [see Figs. 2(a)–2(c)]. In the same reasoning, close to the $AABB$ tetramer crossing, the hexamer $AAABBB$ is a weakly bound DDD state which splits into three dimers when the dimer-dimer attraction changes to repulsion, resulting in the same threshold value.

In the above discussion, we have integrated out the internal degrees of freedom of the dimers, replacing them by elementary pointlike bosons. In fact, the DD zero crossing that we observe for $a_{AB} \approx 10a_{BB}$ is a nonperturbative phenomenon resulting from a competition between strong repulsive and attractive interatomic forces among four individual atoms. These interactions are strong since the corresponding scattering lengths are comparable to the typical atomic de Broglie wavelengths $\sim 1/a_{AB}$. We emphasize that this cancellation is achieved only for two dimers. For three dimers, it is incomplete and there is a residual effective three-dimer force of range $\sim a_{AB}$ (distance where the dimers start touching one another). In the many-body problem, this higher order force may compete with the dimer-dimer interaction (if it is not completely zero) or even become dominant. In principle, one can also discuss higher order effects of this type at the DB zero crossing in a DB mixture, but they are expected to be subleading since the DD and BB interactions remain finite. In the remainder of this Rapid Communication, we thus concentrate on the population-balanced case.

In order to characterize the effective three-dimer interaction, we follow the method developed previously in one dimension [9]. Namely, we analyze the behavior of the hexamer energy just below the tetramer threshold. If the tetramer binding energy $E_{DD} = E_{AABB} - 2E_{AB}$ is much smaller than E_{AB} , the dimer-dimer interaction can be considered pointlike and the relative DD wave function can be approximated by $\phi(r) \propto K_0(\kappa r)$, where $\kappa = \sqrt{-2mE_{DD}/\hbar^2}$ is the inverse size of the tetramer. Similarly, the $AAABBB$ hexamer under these conditions reduces to the well-studied problem of three pointlike bosons [41,47–52], according to which the ground-state hexamer binding energy $E_{DDD} = E_{AAABBB} - 3E_{AB}$ should satisfy [51,52]

$$E_{DDD}/|E_{DD}| = -16.5226874. \quad (2)$$

We expect the ratio $E_{DDD}/|E_{DD}|$ to reach the zero-range limit (2) as we approach the dimer-dimer zero crossing, i.e., as

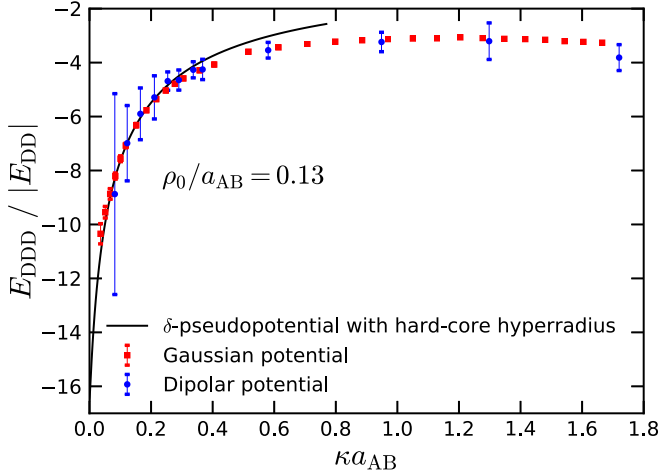


FIG. 3. The hexamer-to-tetramer binding energy ratio $E_{DDD}/|E_{DD}|$ as a function of κa_{AB} . The solid line is the result of the zero-range model with the hard-core hyper-radius constraint at $\rho_0 = 0.13a_{AB}$.

$\kappa a_{AB} \rightarrow 0$. In Fig. 3, we plot $E_{DDD}/|E_{DD}|$ versus κa_{AB} and indeed see a tendency toward the value (2) although the effects of the finite size of the dimers and their internal degrees of freedom, that we have neglected in the zero-range model, are obviously important. The fact that the hexamer energy lies above the limit (2) points to an effective three-dimer repulsive force. We note again that the values of the ratio $E_{DDD}/|E_{DD}|$ obtained for Gaussian and dipolar potentials are quite close to each other for all values of a_{AB} , suggesting a certain universality of this problem and a relative unimportance of the long-range interaction tails.

In order to quantify the three-dimer interaction observed in Fig. 3, we extend the model of three pointlike dimers by requiring that the three-dimer wave function vanishes at a hyper-radius ρ_0 . For three dimers, with coordinates \mathbf{r}_1 , \mathbf{r}_2 , and \mathbf{r}_3 , the hyper-radius is defined as $\rho = \sqrt{x^2 + y^2}$, where $\mathbf{x} = (2\mathbf{r}_3 - \mathbf{r}_1 - \mathbf{r}_2)/\sqrt{3}$ and $\mathbf{y} = \mathbf{r}_1 - \mathbf{r}_2$ are the Jacobi coordinates. Clearly, for this minimalistic model $E_{DDD}/|E_{DD}|$ is a function of the ratio $\kappa\rho_0$, relating the three- and two-dimer interaction strengths. Given the isotropic form of the three-body constraint in the hyper-radial space, a natural way of solving this problem is to use the adiabatic hyperspherical method. Kartavtsev and Malykh [52] discussed this method in detail and applied it to the $\rho_0 = 0$ limit of our problem, i.e., the case of no three-body interaction. The only modification of their procedure, to account for finite ρ_0 , is to set the hyper-radial channel functions to zero at $\rho = \rho_0$. In this way, we obtain the ratio $E_{DDD}/|E_{DD}|$ as a function of $\kappa\rho_0$. We then treat ρ_0 as a constant (independent of E_{DD}) determined by fitting the DMC and SVM data in the $\kappa a_{AB} < 0.4$ range. By minimizing χ^2 , we obtain $\rho_0 = 0.13a_{AB}$.

The inclusion of the three-body hard-core constraint, even corresponding to numerically very small $\kappa\rho_0$, leads to a spectacular deviation from Eq. (2). This interesting effect is due to an enhancement of the three-dimer interaction by strong two-dimer correlations. Indeed, in the absence of two-body interactions, the three-body scattering in two dimensions is equivalent to the four-dimensional two-body scattering on a

short-range potential. The corresponding hyper-radial wave function for ρ larger than the support of the potential, but smaller than the de Broglie wave length, is proportional to $1 - \rho_0^2/\rho^2$. The same scattering effect in the first Born approximation (and the same mean-field interaction shift) is attained by using the three-body potential $V_3(\mathbf{r}_1, \mathbf{r}_2, \mathbf{r}_3) = 3\pi^2(\hbar^2\rho_0^2/m)\delta(\mathbf{r}_1 - \mathbf{r}_2)\delta(\mathbf{r}_2 - \mathbf{r}_3)$. Naively, we expect the leading small- ρ_0 correction to Eq. (2) to behave as $(\kappa\rho_0)^2$ as if the three dimers without two-body interactions were externally confined to a surface $\sim 1/\kappa^2$. However, in our case two-dimer correlations are strong and the three-dimer wave function is logarithmically enhanced at short hyper-radii [52]. More precisely, by using arguments of Ref. [52] one can show that the hyper-radial wave function at distances $\rho \ll 1/\kappa$ behaves as $\ln^3(\kappa\rho) - \rho_0^2 \ln^6(\kappa\rho_0)\rho^{-2} \ln^{-3}(\kappa\rho)$ and the leading-order correction to Eq. (2) behaves as $\sim(\kappa\rho_0)^2 \ln^6(\kappa\rho_0)$, representing a noticeable enhancement compared to the case of no two-body interaction.

Promising candidates for observing the predicted cluster states are bosonic dipolar molecules characterized by large and tunable dipolar lengths which, at large electric fields, tend to $r_0 = 5 \times 10^{-6}$ m for $^{87}\text{Rb}^{133}\text{Cs}$ [53,54], $r_0 = 2 \times 10^{-5}$ m for $^{23}\text{Na}^{87}\text{Rb}$ [55,56], and $r_0 = 6 \times 10^{-5}$ m for $^7\text{Li}^{133}\text{Cs}$ [57]. Fermionic $^{87}\text{Rb}^{40}\text{K}$ [58,59] and $^{23}\text{Na}^{40}\text{K}$ [60–62] molecules ($r_0 = 7 \times 10^{-7}$ m and $r_0 = 7 \times 10^{-6}$, respectively) could be turned into bosons by choosing another isotope of K. The interlayer distance, fixed by the laser wavelength, has typical values of $h \approx (2-5) \times 10^{-7}$ m, which is thus sufficient for observing the few-body bound states that we predict for ratios $h/r_0 > 0.8$.

A subject of further work is to generalize these findings to the many-body problem when a new scale (density n) comes into play. It is important to understand how the two- and three-body effects correlate with each other as one passes through the dimer-dimer zero crossing. Although we find no qualitative difference between the dipolar and Gaussian models in our few-body results, the long-range tails will be important when the quantity nr_0 becomes comparable to the inverse healing length (which is where the dipolar condensate becomes rotonized). For bilayer dipoles, the relevant region of parameters is close to the dimer-dimer zero crossing, which we predict to be at $h/r_0 \approx 1.1$. Finally, it is instructive to consider a simpler model of elementary bosons with (possibly exotic) finite-range interactions and investigate whether finite-range effects can be absorbed into an effective three-body interaction. Systematic calculations of the trimer-to-dimer binding energy ratio (see Ref. [48]) could then serve as a tool for characterizing this effective force.

To summarize, we have studied few-body clusters $A_N B_M$ with $N \leq M \leq 3$ in a two-dimensional Bose-Bose mixture using different (long-range dipolar and short-range Gaussian) intraspecies repulsion and interspecies attraction models. In both cases, the intraspecies scattering length $a_{AA} = a_{BB}$ is of the order of the potential ranges, whereas we tune a_{AB} by adjusting the AB attractive potential (or the interlayer distance in the bilayer setup). We find that for $a_{AB} \gg a_{BB}$ all considered clusters are (weakly) bound and their energies are independent of the interaction model. As the ratio a_{AB}/a_{BB} decreases, the increasing intraspecies repulsion pushes the clusters upwards in energy and eventually breaks them up into N dimers and

$M - N$ free B atoms. In the population balanced case ($N = M$), this happens at $a_{AB}/a_{BB} \approx 10$, where the dimer-dimer attraction changes to repulsion. By studying the $AAABBB$ hexamer near the dimer-dimer zero crossing, we find that it very much behaves like a system of three pointlike particles (dimers) characterized by an effective three-dimer repulsion. A dipolar system in a bilayer geometry can thus exhibit the tunability and mechanical stability necessary for observing dilute liquids and supersolid phases.

This study has been partially supported by funding from the Spanish MINECO (Grant No. FIS2017-84114-C2-1-P). The Barcelona Supercomputing Center (The Spanish National Supercomputing Center—Centro Nacional de Supercomputación) is acknowledged for the provided computational facilities (Grant No. RES-FI-2019-2-0033). G.G. acknowledges a fellowship from CONACYT (México). D.S.P. acknowledges support from ANR Grant Droplets No. ANR-19-CE30-0003-02.

- [1] H. Kadau, M. Schmitt, M. Wenzel, C. Wink, T. Maier, I. Ferrier-Barbut, and T. Pfau, Observing the Rosensweig instability of a quantum ferrofluid, *Nature (London)* **530**, 194 (2016).
- [2] M. Schmitt, M. Wenzel, F. Böttcher, I. Ferrier-Barbut, and T. Pfau, Self-bound droplets of a dilute magnetic quantum liquid, *Nature (London)* **539**, 259 (2016).
- [3] I. Ferrier-Barbut, H. Kadau, M. Schmitt, M. Wenzel, and T. Pfau, Observation of Quantum Droplets in a Strongly Dipolar Bose Gas, *Phys. Rev. Lett.* **116**, 215301 (2016).
- [4] L. Chomaz, S. Baier, D. Petter, M. J. Mark, F. Wächtler, L. Santos, and F. Ferlaino, Quantum-Fluctuation-Driven Crossover from a Dilute Bose-Einstein Condensate to a Macrodroplet in a Dipolar Quantum Fluid, *Phys. Rev. X* **6**, 041039 (2016).
- [5] C. R. Cabrera, L. Tanzi, J. Sanz, B. Naylor, P. Thomas, P. Cheiney, and L. Tarruell, Quantum liquid droplets in a mixture of Bose-Einstein condensates, *Science* **359**, 301 (2018).
- [6] G. Semeghini, G. Ferioli, L. Masi, C. Mazzinghi, L. Wolswijk, F. Minardi, M. Modugno, G. Modugno, M. Inguscio, and M. Fattori, Self-Bound Quantum Droplets of Atomic Mixtures in Free Space, *Phys. Rev. Lett.* **120**, 235301 (2018).
- [7] G. Ferioli, G. Semeghini, L. Masi, G. Giusti, G. Modugno, M. Inguscio, A. Gallemí, A. Recati, and M. Fattori, Collisions of Self-Bound Quantum Droplets, *Phys. Rev. Lett.* **122**, 090401 (2019).
- [8] A. Pricoupenko and D. S. Petrov, Dimer-dimer zero crossing and dilute dimerized liquid in a one-dimensional mixture, *Phys. Rev. A* **97**, 063616 (2018).
- [9] G. Guijarro, A. Pricoupenko, G. E. Astrakharchik, J. Boronat, and D. S. Petrov, One-dimensional three-boson problem with two- and three-body interactions, *Phys. Rev. A* **97**, 061605(R) (2018).
- [10] D.-W. Wang, M. D. Lukin, and E. Demler, Quantum Fluids of Self-Assembled Chains of Polar Molecules, *Phys. Rev. Lett.* **97**, 180413 (2006).
- [11] D.-W. Wang, Quantum Phase Transitions of Polar Molecules in Bilayer Systems, *Phys. Rev. Lett.* **98**, 060403 (2007).
- [12] C. Trefzger, C. Menotti, B. Capogrosso-Sansone, and M. Lewenstein, Ultracold dipolar gases in optical lattices, *J. Phys. B: At., Mol. Opt. Phys.* **44**, 193001 (2011).
- [13] D. H. J. O'Dell, S. Giovanazzi, and G. Kurizki, Rotons in Gaseous Bose-Einstein Condensates Irradiated by a Laser, *Phys. Rev. Lett.* **90**, 110402 (2003).
- [14] L. Santos, G. V. Shlyapnikov, and M. Lewenstein, Roton-Maxon Spectrum and Stability of Trapped Dipolar Bose-Einstein Condensates, *Phys. Rev. Lett.* **90**, 250403 (2003).
- [15] Z.-K. Lu, Y. Li, D. S. Petrov, and G. V. Shlyapnikov, Stable Dilute Supersolid of Two-Dimensional Dipolar Bosons, *Phys. Rev. Lett.* **115**, 075303 (2015).
- [16] L. Tanzi, E. Lucioni, F. Famà, J. Catani, A. Fioretti, C. Gabbanini, R. N. Bisset, L. Santos, and G. Modugno, Observation of a Dipolar Quantum Gas with Metastable Supersolid Properties, *Phys. Rev. Lett.* **122**, 130405 (2019).
- [17] L. Chomaz, D. Petter, P. Ilzhöfer, G. Natale, A. Trautmann, C. Politi, G. Durastante, R. M. W. van Bijnen, A. Patscheider, M. Sohmen, M. J. Mark, and F. Ferlaino, Long-Lived and Transient Supersolid Behaviors in Dipolar Quantum Gases, *Phys. Rev. X* **9**, 021012 (2019).
- [18] F. Böttcher, J.-N. Schmidt, M. Wenzel, J. Hertkorn, M. Guo, T. Langen, and T. Pfau, Transient Supersolid Properties in an Array of Dipolar Quantum Droplets, *Phys. Rev. X* **9**, 011051 (2019).
- [19] L. Tanzi, S. M. Roccuzzo, E. Lucioni, F. Famà, A. Fioretti, C. Gabbanini, G. Modugno, A. Recati, and S. Stringari, Supersolid symmetry breaking from compressional oscillations in a dipolar quantum gas, *Nature (London)* **574**, 382 (2019).
- [20] M. Guo, F. Böttcher, J. Hertkorn, J.-N. Schmidt, M. Wenzel, H.-P. Büchler, T. Langen, and T. Pfau, The low-energy Goldstone mode in a trapped dipolar supersolid, *Nature (London)* **574**, 386 (2019).
- [21] G. Natale, R. M. W. van Bijnen, A. Patscheider, D. Petter, M. J. Mark, L. Chomaz, and F. Ferlaino, Excitation Spectrum of a Trapped Dipolar Supersolid and Its Experimental Evidence, *Phys. Rev. Lett.* **123**, 050402 (2019).
- [22] H.-P. Büchler, E. Demler, M. Lukin, A. Micheli, N. Prokof'ev, G. Pupillo, and P. Zoller, Strongly Correlated 2D Quantum Phases with Cold Polar Molecules: Controlling the Shape of the Interaction Potential, *Phys. Rev. Lett.* **98**, 060404 (2007).
- [23] G. E. Astrakharchik, J. Boronat, I. L. Kurbakov, and Y. E. Lozovik, Quantum Phase Transition in a Two-Dimensional System of Dipoles, *Phys. Rev. Lett.* **98**, 060405 (2007).
- [24] A. Macia, G. E. Astrakharchik, F. Mazzanti, S. Giorgini, and J. Boronat, Single-particle versus pair superfluidity in a bilayer system of dipolar bosons, *Phys. Rev. A* **90**, 043623 (2014).
- [25] G. E. Astrakharchik, R. E. Zillich, F. Mazzanti, and J. Boronat, Gapped spectrum in pair-superfluid bosons, *Phys. Rev. A* **94**, 063630 (2016).
- [26] J. Nespolo, G. E. Astrakharchik, and A. Recati, Andreev-Bashkin effect in superfluid cold gases mixtures, *New J. Phys.* **19**, 125005 (2017).

- [27] A. Safavi-Naini, Ş. G. Söyler, G. Pupillo, H. R. Sadeghpour, and B. Capogrosso-Sansone, Quantum phases of dipolar bosons in bilayer geometry, *New J. Phys.* **15**, 013036 (2013).
- [28] Note that the analogous integral in the bitube geometry is finite [see, for example, B. Wunsch, N. T. Zinner, I. B. Mekhov, S.-J. Huang, D.-W. Wang, and E. Demler, Few-Body Bound States in Dipolar Gases and Their Detection, *Phys. Rev. Lett.* **107**, 073201 (2011)].
- [29] V. I. Yudson, M. G. Rozman, and P. Reineker, Bound states of two particles confined to parallel two-dimensional layers and interacting via dipole-dipole or dipole-charge laws, *Phys. Rev. B* **55**, 5214 (1997).
- [30] S.-M. Shih and D.-W. Wang, Pseudopotential of an interaction with a power-law decay in two-dimensional systems, *Phys. Rev. A* **79**, 065603 (2009).
- [31] J. R. Armstrong, N. T. Zinner, D. V. Fedorov, and A. S. Jensen, Bound states and universality in layers of cold polar molecules, *Europhys. Lett.* **91**, 16001 (2010).
- [32] M. Klawunn, A. Pikovski, and L. Santos, Two-dimensional scattering and bound states of polar molecules in bilayers, *Phys. Rev. A* **82**, 044701 (2010).
- [33] M. A. Baranov, A. Micheli, S. Ronen, and P. Zoller, Bilayer superfluidity of fermionic polar molecules: Many-body effects, *Phys. Rev. A* **83**, 043602 (2011).
- [34] A. G. Volosniev, D. V. Fedorov, A. S. Jensen, and N. T. Zinner, Model Independence in Two Dimensions and Polarized Cold Dipolar Molecules, *Phys. Rev. Lett.* **106**, 250401 (2011).
- [35] B. Simon, The bound state of weakly coupled Schrödinger operators in one and two dimensions, *Ann. Phys.* **97**, 279 (1976).
- [36] A. G. Volosniev, D. V. Fedorov, A. S. Jensen, and N. T. Zinner, Few-body bound-state stability of dipolar molecules in two dimensions, *Phys. Rev. A* **85**, 023609 (2012).
- [37] C. Ticknor, Two-dimensional dipolar scattering, *Phys. Rev. A* **80**, 052702 (2009).
- [38] J. Boronat and J. Casulleras, Monte Carlo analysis of an interatomic potential for He, *Phys. Rev. B* **49**, 8920 (1994).
- [39] Y. Suzuki and K. Varga, *Stochastic Variational Approach to Quantum-Mechanical Few-Body Problems* (Springer, Berlin, 1998).
- [40] B. Bazak, M. Eliyahu, and U. van Kolck, Effective field theory for few-boson systems, *Phys. Rev. A* **94**, 052502 (2016).
- [41] I. V. Brodsky, M. Yu. Kagan, A. V. Klaptsov, R. Combescot, and X. Leyronas, Exact diagrammatic approach for dimer-dimer scattering and bound states of three and four resonantly interacting particles, *Phys. Rev. A* **73**, 032724 (2006).
- [42] L. Pricoupenko and P. Pedri, Universal (1+2)-body bound states in planar atomic waveguides, *Phys. Rev. A* **82**, 033625 (2010).
- [43] F. F. Bellotti, T. Frederico, M. T. Yamashita, D. V. Fedorov, A. S. Jensen, and N. T. Zinner, Scaling and universality in two dimensions: Three-body bound states with short-ranged interactions, *J. Phys. B: At. Mol. Opt. Phys.* **44**, 205302 (2011).
- [44] B. Bazak and D. S. Petrov, Energy of N two-dimensional bosons with zero-range interactions, *New J. Phys.* **20**, 023045 (2018).
- [45] T. Ren and I. Aleiner, Three-boson bound states in three dimensions, *Phys. Rev. B* **95**, 045401 (2017).
- [46] B. Bazak and D. S. Petrov, Stable p -Wave Resonant Two-Dimensional Fermi-Bose Dimers, *Phys. Rev. Lett.* **121**, 263001 (2018).
- [47] L. W. Bruch and J. A. Tjon, Binding of three identical bosons in two dimensions, *Phys. Rev. A* **19**, 425 (1979).
- [48] Sadhan K. Adhikari, A. Delfino, T. Frederico, I. D. Goldman, and Lauro Tomio, Efimov and Thomas effects and the model dependence of three-particle observables in two and three dimensions, *Phys. Rev. A* **37**, 3666 (1988).
- [49] E. Nielsen, D. V. Fedorov, and A. S. Jensen, Three-body halos in two dimensions, *Phys. Rev. A* **56**, 3287 (1997).
- [50] E. Nielsen, D. V. Fedorov, and A. S. Jensen, Structure and occurrence of three-body halos in two dimensions, *Few-Body Syst.* **27**, 15 (1999).
- [51] H.-W. Hammer and D. T. Son, Universal Properties of Two-Dimensional Boson Droplets, *Phys. Rev. Lett.* **93**, 250408 (2004).
- [52] O. I. Kartavtsev and A. V. Malykh, Universal low-energy properties of three two-dimensional bosons, *Phys. Rev. A* **74**, 042506 (2006).
- [53] T. Takekoshi, L. Reichsöllner, A. Schindewolf, J. M. Hutson, C. R. Le Sueur, O. Dulieu, F. Ferlaino, R. Grimm, and H.-C. Nägerl, Ultracold Dense Samples of Dipolar RbCs Molecules in the Rovibrational and Hyperfine Ground State, *Phys. Rev. Lett.* **113**, 205301 (2014).
- [54] P. K. Molony, P. D. Gregory, Z. Ji, B. Lu, M. P. Köpinger, C. R. Le Sueur, C. L. Blackley, J. M. Hutson, and S. L. Cornish, Creation of Ultracold $^{87}\text{Rb}^{133}\text{Cs}$ Molecules in the Rovibrational Ground State, *Phys. Rev. Lett.* **113**, 255301 (2014).
- [55] M. Guo, B. Zhu, B. Lu, X. Ye, F. Wang, R. Vexiau, N. Bouloufa-Maafa, G. Quémener, O. Dulieu, and D. Wang, Creation of an Ultracold Gas of Ground-State Dipolar $^{23}\text{Na}^{87}\text{Rb}$ Molecules, *Phys. Rev. Lett.* **116**, 205303 (2016).
- [56] M. Guo, X. Ye, J. He, G. Quémener, and D. Wang, High-resolution internal state control of ultracold $^{23}\text{Na}^{87}\text{Rb}$ molecules, *Phys. Rev. A* **97**, 020501(R) (2018).
- [57] J. Deiglmayr, A. Grochola, M. Repp, O. Dulieu, R. Wester, and M. Weidemüller, Permanent dipole moment of LiCs in the ground state, *Phys. Rev. A* **82**, 032503 (2010).
- [58] S. A. Moses, J. P. Covey, M. T. Miecnikowski, B. Yan, B. Gadway, J. Ye, and D. S. Jin, Creation of a low-entropy quantum gas of polar molecules in an optical lattice, *Science* **350**, 659 (2015).
- [59] L. De Marco, G. Valtolina, K. Matsuda, W. G. Tobias, J. P. Covey, and J. Ye, A degenerate Fermi gas of polar molecules, *Science* **363**, 853 (2019).
- [60] J. W. Park, S. A. Will, and M. W. Zwierlein, Ultracold Dipolar Gas of Fermionic $^{23}\text{Na}^{40}\text{K}$ Molecules in Their Absolute Ground State, *Phys. Rev. Lett.* **114**, 205302 (2015).
- [61] J. W. Park, Z. Z. Yan, H. Loh, S. A. Will, and M. W. Zwierlein, Second-scale nuclear spin coherence time of ultracold $^{23}\text{Na}^{40}\text{K}$ molecules, *Science* **357**, 372 (2017).
- [62] H. Yang, D.-C. Zhang, L. Liu, Y.-X. Liu, J. Nan, B. Zhao, and J.-W. Pan, Observation of magnetically tunable Feshbach resonances in ultracold $^{23}\text{Na}^{40}\text{K} + ^{40}\text{K}$ collisions, *Science* **363**, 261 (2019).